Biofilm 8 (2024) 100214

Contents lists available at ScienceDirect

Biofilm

journal homepage: www.sciencedirect.com/journal/biofilm

Intra-strain colony biofilm heterogeneity in uropathogenic *Escherichia coli* and the effect of the NlpI lipoprotein

Hamilton D. Green [a], Gerald T. Van Horn [a,c], Timothy Williams [a], Allison Eberly [a], Grace H. Morales [a], Robert Mann [a], Indiana M. Hauter [a], Maria Hadjifrangiskou [a,b,c], Jonathan E. Schmitz [a,b,c,*]

[a] *Division of Molecular Pathogenesis, Department of Pathology, Microbiology & Immunology, Vanderbilt University Medical Center, Nashville, TN, 37232, USA*
[b] *Vanderbilt Institute for Infection, Immunology & Inflammation, Vanderbilt University Medical Center, Nashville, TN, USA*
[c] *Center for Personalized Microbiology, Department of Pathology, Microbiology & Immunology, Vanderbilt University Medical Center, Nashville, TN, USA*

ARTICLE INFO

Keywords:
Uropathogenic *Escherichia coli*
Bacterial heterogeneity
Congo red
Colony biofilm
NlpI

ABSTRACT

Biofilm growth facilitates the interaction of uropathogenic *Escherichia coli* (UPEC) with the host environment. The extracellular polymeric substances (EPS) of UPEC biofilms are composed prominently of curli amyloid fiber and cellulose polysaccharide. When the organism is propagated as a colony biofilm on agar media, these macromolecules can generate pronounced macroscopic structures. Moreover, curli/cellulose associate tightly with Congo red, generating a characteristic pink-to-red staining pattern when the media is supplemented with this dye. Among different clinical isolates of UPEC, changes in the abundance of curli/cellulose can lead to diverse colony biofilm phenotypes on a strain-by-strain basis. Nevertheless, for any given isolate, these phenotypes are classically homogenous throughout the colony biofilm. Here, we report that a subset of clinical UPEC isolates display heterogenous 'peppermint' colony biofilms, with distinct pale and red subpopulations. Through isolation of these subpopulations and whole genome sequencing, we demonstrate various emergent mutations associated with the phenomenon, including within the gene encoding the outer membrane lipoprotein *nlpI*. Deletion of *nlpI* within independent strain-backgrounds increased biofilm rugosity, while its overexpression induced the peppermint phenotype. Upregulation of EPS-associated proteins and transcripts was likewise observed in the absence of *nlpI*. Overall, these results demonstrate that EPS elaboration in UPEC is impacted by *nlpI*. More broadly, this phenomenon of intra-strain colony biofilm heterogeneity may be leveraged as a tool to identify additional members within the broad collection of genes that regulate or otherwise affect biofilm formation.

1. Introduction

Bacteria can form multicellular communities, collectively termed biofilms, which are encased in extracellular polymeric substances (EPS). Biofilms create tremendous burdens for the healthcare system, especially in the context of difficult-to-treat infections [1,2]. These include urinary tract infections (UTIs), for which the most common agent is uropathogenic *E. coli* (UPEC). Two of the most prominent EPS components of UPEC biofilms are curli (proteinaceous) amyloid fibers, as well as phosphoethanolamine (pEtN) cellulose [3–6]. The elaboration of EPS contributes to the pathogenesis and persistence of UPEC, including in their adherence to urothelial cells [4] and in the context of antibiotic treatment [7–9]. EPS can hamper antibiotic penetration into a biofilm, blocking bacterial killing and contributing to antibiotic failure [10]. Overall, understanding the mechanisms of EPS elaboration is paramount to efforts to combat biofilm infections.

Even within a bacterial species, different modalities of biofilm-phase growth are possible, depending on the environmental milieu. For instance, these include liquid submerged biofilms that proliferate on solid surfaces [11]; surface associated biofilms at a liquid-air interface [12,13]; as well as pellicle biofilms proliferating at this same level [14,15]. In the case of UPEC, a common modality for studying biofilm growth entails the generation of *colony biofilms,* with the traditional process summarized in Fig. 1 [16,17]. Here, *E. coli* is inoculated onto an agar media (YESCA - yeast extract, casamino acids), stimulating the elaboration of curli/cellulose and the development of surface rugosity.

Abbreviations: UPEC, Uropathogenic Escherichia coli; EPS, Extra Polymeric Substances; YESCA, Yeast Extract Casamino Acid; CR, Congo Red.

* Corresponding author. Department of Pathology, Microbiology & Immunology, Vanderbilt University Medical Center, Nashville, TN, 37232, USA.
E-mail address: jonathan.e.schmitz@vumc.org (J.E. Schmitz).

https://doi.org/10.1016/j.bioflm.2024.100214
Received 19 March 2024; Received in revised form 25 June 2024; Accepted 9 July 2024
Available online 17 July 2024

The presence of EPS can be accentuated further through the addition of Congo red (CR) dye, which preferentially binds curli and cellulose [16–19]. Notably, the morphology of *E. coli* colony biofilms on YESCA-CR agar can differ from isolate to isolate – that is, on an *inter-strain* basis – with great variability among wild-type strains [20]. Qualitative schema has been developed to categorize *E. coli* colony biofilms in terms of surface rugosity and CR-uptake (i.e., 'redness') [18,21,22].

In addition to inter-strain heterogeneity, an additional (but under-studied) phenomenon for UPEC colony biofilms is the development of *intrastrain* heterogeneity. Broadly defined, intra-strain biofilm heterogeneity occurs when initially clonal bacteria proliferate into biofilms with spatial subpopulations that differ phenotypically and/or genotypically [23–25]. Such subpopulations can emerge due to the accumulation of genetic mutations, gene-expression changes in response to localized environmental stimuli or bet-hedging responses [25,26]. Temperature, pH, oxygen gradients, and nutrient availability have been associated with the induction of such heterogeneity [25,27,28]. Across various mechanisms, intra-strain heterogeneity can contribute to the long-term persistence of bacterial pathogens during human infection [21–23].

UPEC is among the most frequently encountered organisms within clinical laboratories, largely due to the high volume of diagnostic urine cultures [29]. Among such strains, however, the prevalence and dynamics of biofilm heterogeneity remain poorly defined. In this context, we profiled the colony biofilm phenotypes of a large collection of clinical UPEC strains obtained from diagnostic care, with an emphasis on both inter- and intra-strain heterogeneity, including the emergence of distinct subpopulations within individual colony biofilms. Not surprisingly, from isolate to isolate, we observed significant inter-strain diversity in terms of rugosity and CR-uptake. At the same time, we also observed that a subset of strains demonstrated additional intra-strain diversity, with colony biofilms exhibiting (what we term) a *peppermint* phenotype – that is, the visual appearance of genetically stable subpopulations and corresponding striations on the edge of colony biofilms. We harnessed this phenomenon to identify an additional member of a regulatory network that modulates EPS elaboration in *E. coli*, the outer membrane (OM) protein NlpI, characterizing its role in both a wild-type background and the model strain UTI89. In total, the current work highlights an additional layer of intra-strain complexity in UPEC biofilms, while providing a novel strategy for characterizing their regulation through strains with inherent heterogeneity.

2. Materials and Methods

2.1. Bacterial strains and mutant constructs

All clinical *E. coli* strains utilized in this study were obtained from the diagnostic laboratory at Vanderbilt University Medical Center (designated as 'VUTI' strains). These 514 strains intentionally represented the significant clinical diversity associated with *E. coli* bacteriuria, in terms of patient demographics, collection setting, clinical presentation (e.g., asymptomatic bacteriuria, cystitis, ascending infection), and complicating/comorbid conditions. A complete summary of the clinical parameters associated with each isolate is included in **Supplementary Data 1.** For the model cystitis strain UTI89, gene deletions were constructed with the lambda red recombinase system [30]. For genetic complementation of strains VUTI148 and UTI89, plasmids were

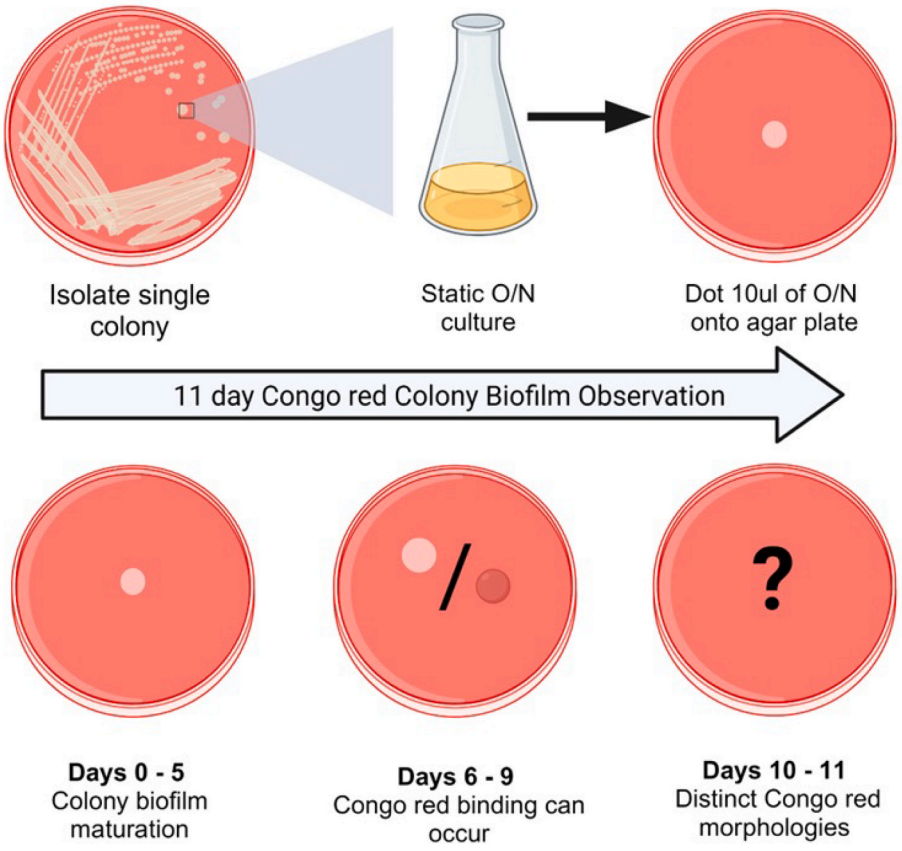

Fig. 1. Evaluating UPEC Colony Biofilms by YESCA-CR Agar. Urinary *E. coli* isolates are first streaked on blood agar plates. Single colonies are then selected and propagated overnight at 37 °C in static liquid culture. 10 μ1 of this overnight culture is inoculated as a patch onto YESCA agar plates supplemented with Congo red dye, which is capable of binding EPS components curli and cellulose. The cultures are allowed to mature for 11 days at room temperature and then observed for colony biofilm morphology.

engineered with the Takara Infusion Cloning Kit.

2.2. Colony biofilm culture

E. coli colony biofilms were generated according to established protocols [16–18,21,22,31,32]. In summary (Fig. 1), each strain was selected from a single colony on blood agar and propagated overnight statically at 37 °C in Luria Broth (pH = 7.4); 10 μl of this liquid culture was inoculated onto Yeast Extract Casamino Acid agar (1.2X concentration) supplemented with CR (40 μg/mL) and bromophenol Blue (20 μg/mL). These cultures developed for 11 days at room temperature and ambient atmosphere, and the resultant colony biofilms were assessed. To isolate emergent subpopulations with distinct colony biofilm phenotypes, the relevant regions were sampled with a sterile inoculating loop, followed by isolation-streaking onto fresh YESCA-CR agar. This process was repeated 3–5 times to ensure the clonality and phenotypic stability of the subpopulation. In each case, both the parent strain and regions of the initial colony biofilm without subpopulation emergence were sub-cultured in parallel, as direct phenotypic comparator and to serve as controls in downstream genomic analysis (section 2.4).

To formulate urine agar-CR plates, pooled urine was obtained commercially (Lee BioSolutions) and sterilized through a 0.22-μm vacuum filtration. It was supplemented with Congo red and bromophenol blue (concentrations described above); these were then added to a molten (autoclaved) agar suspension (4X) to generate a final agar concentration of 1.2X. The urine itself was not autoclaved to avoid any potential thermal decomposition.

2.3. Single-CFU evaluation of subpopulation emergence

For select strains whose colony biofilms demonstrated subpopulation emergence, additional liquid starter-cultures were propagated as above. Following overnight growth, these cultures were diluted to 10^3–10^4 colony forming units per ml (CFU/ml) and plated onto YESCA-CR agar for single-colony isolation. Individual colonies were evaluated for emergent CR-uptake phenotypes that were distinct from the parent/predominant strain. The proportion of colonies with an emergent morphology were evaluated in each case, with data representing three biological replicates. In control experiments, the liquid culture was plated out immediately after its starter-inoculum (without overnight growth).

2.4. Whole genome sequencing and read mapping

Genomic DNA was extracted from *E. coli* VUTI148 (and its colony biofilm subpopulations) with the PureLink Genomic DNA Mini Kit (Invitrogen). These gDNA specimens were submitted to the Microbial Genome Sequencing Center (Pittsburg, PA) for paired-end Illumina sequencing (2 x 151bp). Analysis of the resultant data was performed with the Geneious software package. Following barcode and quality trimming, the parent strain was subjected to *de novo* assembly via the Spades algorithm to generate consensus contigs. Among these sequences, contigs with a length >100 bp and average coverage-depth >50X were concatenated to serve as a reference genome. Subsequently, trimmed reads for each bacterial subpopulation were mapped to this reference and analyzed for emergent mutations. To qualify, the latter had to demonstrate >15X coverage-depth at that locus with >90 % conserved nucleotide identity across individual reads. WGS data from parental VUTI148 and nonemergent regions of the same biofilms were analyzed in the same manner, to ensure that observed mutations were unique to the emergent subpopulation and not artifactual.

2.5. Comparative sequence analysis

For 241/514 *E. coli* strains assessed here, gDNA was extracted and contig-level whole genome sequences were obtained as described above (NCBI BioProject PRJNA819016) [33]. For the *nlpI* and *hfq* loci, nucleotide sequences were extracted via Blastn (v. 2.12.0+). Percent identity (nucleotide and translated amino acid sequences) was compared among the strains mapped to a maximum-likelihood tree built on the shared core genome (using Parsnp v. 1.7.4).

2.6. Proteomic analyses

Relevant bacterial constructs were analyzed by liquid chromatography with tandem mass spectrometry (LC-MS-MS). Large-volume bacterial cultures were propagated overnight in YESCA broth (37°C with shaking), to ensure abundant biomass for downstream extraction. Cultures were pelleted and resuspended in EDTA-PMSF buffer, with 1 h incubation at 4 °C, followed by 3-fold passage through an Emulsiflex. This suspension was subjected to ultracentrifugation (40,000 RPM, 1hr, 4 °C), followed by addition of 0.5 % Sarkosyl to separate inner and outer membrane fractions. Each fraction was resuspended in 1 mL Tris (20 mM, pH 7.4), from which 25 μg total protein was prepared for spectrometry via S-trap columns and tryptic digest (Protifi, according to manufacturer instructions). The resultant peptides were quantitated by 280-nm absorbance (Nanodrop) and 100 ng of each specimen was analyzed by LC-MS-MS on a Q Exactive Plus Orbitrap spectrometer (ThermoFisher). Peptides were autosampled onto a 200 mm × 0.1 mm self-packed analytical column (Jupiter 3 μm, 300 Å), resolved with an aqueous-to-organic gradient over a 90-min acquisition time. Peptides were ionized via direct nanoelectrospray; both the intact masses (MS) and fragmentation patterns (MS/MS) of the peptides were collected with dynamic exclusion to maximize depth of coverage.

The resultant spectra were analyzed in the MaxQuant software package [34], referenced to an *E. coli* UTI89 database (Uniprot) in which common contaminants and reversed versions of each protein were added. Peptide spectral matches were collated, filtered, and visualized in Scaffold. Label-free quantitative comparisons were performed in the MSstats v4.0 statistical analysis package [35] with 3 biological replicates per condition.

2.7. Real-time reverse transcription polymerase chain reaction

To assess relative transcript abundance at EPS-related loci, cultures were propagated overnight statically at room temperature in YESCA media and pelleted. Total RNA was extracted via RNasy Mini Kits (Qiagen) and treated on column with RNase-Free DNase Set (Qiagen). Each RNA specimen was prepared with at least three to six biological replicates, each diluted to two concentrations and analyzed via three technical replicates. Targeted RNA samples and replicates were converted to cDNA via TaqPath™ 1-Step RT-qPCR Master Mix, CG (Applied Biosystems). Followed by real-time reverse transcription polymerase chain reaction (RT-qPCR) conducted on a QuantStudio 3 (Applied Biosystems), with probe/primer sequences summarized in Table S1. Across mutant bacterial constructs, the fold-difference in abundance for each transcript was calculated using the $\Delta\Delta C_t$ method, normalized against *rrsH* (i.e. 16S rRNA) levels and presented relative to the abundance in the wildtype [36].

2.8. Ethics statement

This work with clinically derived bacterial strains was performed under protocols approved by the Vanderbilt University Institutional Review Board.

3. Results

3.1. Intra-strain heterogeneity in the EPS of clinical UPEC isolates

Among wild-type strains of urinary *E. coli*, significant variability can exist in their colony biofilm morphology on YESCA-CR agar, driven

primarily by expression patterns of curli and cellulose [3,37]. These morphological differences include the biofilm's CR-uptake, which determines its gross visual coloration (from white to pink to red). In addition, a subset of CR-philic (pink/red) colony biofilms can demonstrate topologic contours, leading to a *rugose* or *rough* appearance [21]. To investigate the strain-to-strain heterogeneity within UPEC, we leveraged a collection of 514 urinary *E. coli* isolates obtained from diagnostic cultures at Vanderbilt University medical center. Not surprisingly, these wildtype strains demonstrated colony biofilm morphotypes across the spectrum previously described [21,37], including: smooth and white, smooth and CR-philic, and rugose and CR-philic (Fig. 2A). Given the observed continuum of *redness* across biofilms in the latter two groups – especially with the large number of isolates characterized for this study – pink/red colonies are classified together here as 'CR-philic'. (Images of all strains are depicted **Supplementary Data 2.**) Across these morphotypes, most strains (404/514, 78.6 %) demonstrated a traditional homogenous appearance, with uniform CR-staining and rugosity over the surface of the colony biofilm.

Interestingly, a significant minority of strains (110/514, 21.4 %) consistently displayed distinct intra-strain heterogeneity in their YESCA-CR morphology. Grossly, these heterogeneous morphologies could be binned into two distinct classes, which we have colloquially termed 'dew drop' (48/514, 9.3 %) and 'peppermint' (62/514, 12.1 %) colony biofilms. In the dew drop, numerous subpopulations would develop on top of the surface of parental colony biofilms (Fig. 2B), each demonstrating less prominent CR-uptake. In peppermint colony biofilms, one or more macroscopic regions would emerge as slices around the circumference of the biofilm (Fig. 2C), with either increased or decreased rugosity/CR-uptake relative to the predominant parental phenotype. Overall, these observations demonstrate that colony biofilms of many wild-type urinary *E. coli* strains do not conform to traditional homogeneous morphotypes.

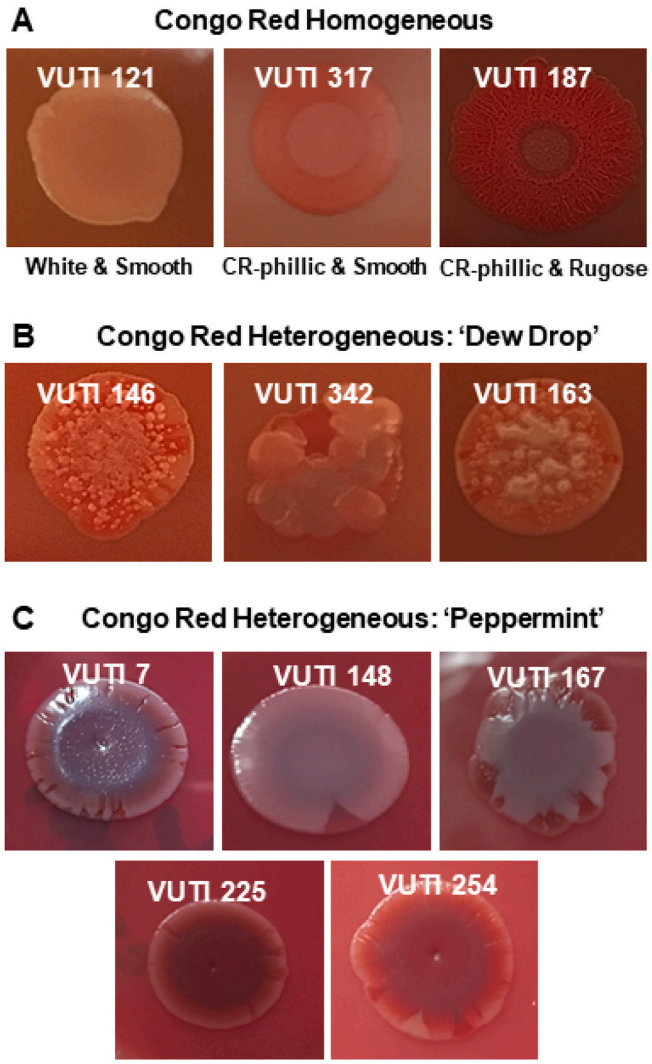

Fig. 2. *E. coli* Colony Biofilm Phenotypes. Representative clinical isolates are depicted here that generate different phenotypic patterns of colony-biofilm growth on YESCA-CR agar. **[A]** Homogenous colony biofilm phenotypes: smooth and white (upper left); smooth and CR-philic (upper middle); rough and CR-philic (upper right). Heterogenous colony biofilms: **[B]** *Dew-drop* colony biofilms; **[C]** *Peppermint* colony biofilms.

For subsequent work in the current manuscript, we focus on the peppermint phenomenon and its underlying genetic basis. This decision was motivated by two factors. First, the diversity of emergent phenotypes for the peppermint subpopulations was notable, including the common emergence of subpopulations with increased EPS elaboration. This contrasts with the appearance of dew-drop subpopulations that exhibit reduced CR-staining. Accordingly, we chose to focus on the dynamics of enhanced CR-staining in peppermint subpopulations, especially considering that it serves as an indicator of curli and cellulose abundance (notable host-interaction factors) [16–18]. Moreover, when reviewing available metadata on the source-patients, we observed a trend between peppermint biofilm strains and patients with a documented history of recurrent UTI (rUTI), as opposed to isolated infections (odds ratio = 2.18, 95 % CI: 0.92–5.19; Fig. S1). Admittedly, we view this clinical finding (based on retrospective chart review and limited sample size) as preliminary, and believe future studies are needed to establish the pathogenetic implications of peppermint colony biofilms (see *Conclusion* for additional discussion). Nevertheless, this combination of factors leads us to prioritize the peppermint phenomenon for further investigation, while acknowledging that defining the basis of dew-drop heterogeneity is also an attractive target for additional research.

3.2. Additional phenotypic characterization of peppermint biofilms

Before exploring the genetic basis of the peppermint phenomenon, we first sought to better define conditions under which these subpopulations emerge. For instance, this includes when/where (physically) biofilm heterogeneity arises for peppermint strains. As a colony biofilm expands radially from its inoculated circumference, the emergence of a subpopulation is macroscopically apparent at a given spatiotemporal location on the agar surface. In fact, both across and within individual peppermint strains, the radial distance at which a peppermint *slice* can emerge is variable. Some of these subpopulations are apparent immediately adjacent to the location of the initial inoculum, while others do not appear until the colony biofilm has already expanded beyond this point, suggesting their emergence on the plate itself. In theory, however, cellular subpopulations could theoretically arise either/both within the maturing colony biofilm itself (i.e., on the agar surface) or within the colony-derived liquid culture from which the biofilm was initially spotted as a 10-μl inoculum. Conversely, on the level of individual bacterial cells, a subpopulation could arise that fails to proliferate/compete to the point of a macroscopically discrete region.

To evaluate these issues, additional experiments were conducted with several peppermint strains (VUTI7, VUTI225, VUTI148) that each displayed emergent subpopulations with increased CR-uptake, relative to the predominant parental morphology. Here, liquid starter-cultures were diluted onto YESCA-CR agar to generate individual colonies (each derived from a single bacteria), rather than a traditional 10-μl patch (containing on the order of ~10^7 cells). While most of these colonies demonstrated the predominant biofilm morphotype of their parent strain, a minority displayed an emergent CR-uptake phenotype. On average, the proportion of emergent colonies overlapped between these 3 strains, albeit with substantial variability for each between biological

replicates (Fig. 3A). Interestingly, within a given CFU, the emergent morphologic phenotype could appear either homogenously or heterogeneously. In the latter case, again reminiscent of a peppermint biofilm, a peripheral slice(s) demonstrates the emergent morphology after some initial radial expansion (Fig. 3B). Again, this strongly suggest that subpopulations arise during growth on the agar surface, especially given the colony's single-CFU origin here. Conversely, in the homogenous scenario, subpopulations would have emerged within liquid culture, prior to plating. Of note, homogenous emergent colonies were not observed when the liquid inoculum was not first incubated overnight.

In addition, for VUTI148, the incubation period of the liquid starter-culture was varied prior to plating on YESCA-CR agar as a 10-μl inoculum, followed by the standard 11-day period of colony biofilm maturation. Here, emergent subpopulations were more abundant when the starter culture was incubated for 48 h prior to plating, accumulating during this second day of incubation (Fig. 3C). Combined, these findings demonstrate that a significant minority of wild-type UPEC strains can develop colony biofilms with intra-strain heterogeneity, and that subpopulations can emerge both during sessile growth in the biofilm itself, as well as during liquid-phase planktonic growth.

Finally, we sought to define the colony biofilm behavior of peppermint strains under additional culture conditions. While the conditions utilized above (i.e. YESCA agar with ambient, room-temperature incubation) represent the traditional *in vitro* conditions for propagating/evaluating *E. coli* colony biofilms, we sought to evaluate methodologic variants that simulate additional aspects of the urinary environment. Towards this goal, VUTI 148 was incubated on urine agar supplemented with CR. After incubation at room temperature and ambient atmosphere, VUTI 148 continued to display a peppermint phenotype on urine agar, including subpopulations with increased CR staining (Fig. S2A). These features likewise remained for VUTI 148 when temperature/atmospheric conditions were further varied on urine-CR agar, including 37 °C in a 4 % O_2 hypoxic chamber (Fig. S2B) and 37 °C with 5 % CO_2 supplementation (Fig. S2C). Of note. O_2 levels in the bladder typically range from 4 to 5.5 % in healthy individuals [38]. Overall, these findings indicate that intra-strain heterogeneity in VUTI 148 is not merely a function of the YESCA medium, as it remains under *in vitro* conditions that mimic what UPEC encounters in the bladder.

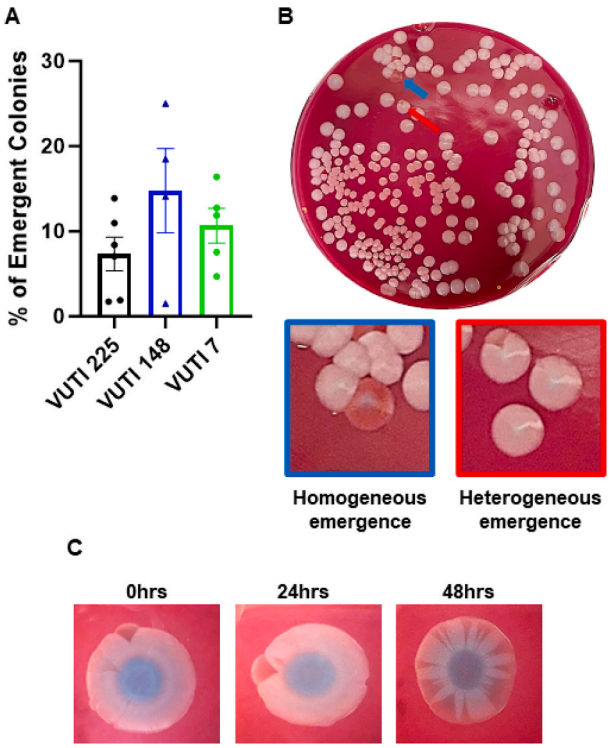

Fig. 3. Emergence of Subpopulations in Liquid Culture. [A] Summarized here, across several *peppermint* strains, is the proportion of colonies displaying an emergent biofilm phenotype following liquid culture and CFU-plating. **[B]** For VUTI148, this image depicts colonies with emergent biofilm phenotypes in a homogeneous (blue/left panel) and heterogeneous (red/right panel) manner. **[C]** VUTI148 colony biofilms (10 μl patch-based, not individual colony-based) are depicted after incubation of liquid cultures for 0 h, 24 h, and 48 h.

3.3. Identification of mutations associated with peppermint heterogeneity

We next sought to explore the basis for intra-strain heterogeneity and subpopulation emergence, focusing on strain VUTI148 (originally isolated from a symptomatic pregnant female with a history of recurrent UTIs). Twenty-six independently emerging subpopulations – each with a stronger CR uptake than parental VUTI148 – were isolated and sub-cultured for several generations on YESCA-CR agar (Fig. 4 and S3). Each such subpopulation was selected from within a distinct peppermint slice. As noted in the Methods (section 2.2), comparator sub-cultures were generated in parallel, selected from regions of the predominant parental biofilm-phenotype. Following sub-culture, the increased CR staining/rugosity of the peppermint-selected subpopulations became homogeneous and remained stable over further sub-cultured generations, suggesting an underlying genetic basis for the phenotypic change (Fig. S3). Likewise, no further emergence of colony biofilm heterogeneity was observed in these subpopulations (including across the various associated genetic mutations described below). By contrast, comparator sub-cultures of the predominant parental phenotype continued to generate subsequent peppermint phenotypes (Fig. 4).

Genomic DNA was isolated from each of the 26 emergent subpopulations and subjected to Illumina sequencing to identify the associated mutation(s), via whole-genomic comparison with parental VUTI148. In each case, the whole-genome sequence of the emergent subpopulation was compared to that of a parental pair – as well as aforementioned subpopulations selected from the predominant parental region – to ensure these emergent polymorphisms were not detected artifactually. A single mutation was identified in 18/26 emergent subpopulations; 2 separate mutations were identified in 4/26 subpopulations; and no emergent mutations were identified in 4/26 subpopulations (summarized in **Supplementary Data 3**). Across all subpopulations, the affected loci encompassed 16 protein-encoding genes and 1 intergenic region; the putative functions of these genes are summarized in Table 1. The most observed mutations, across all subpopulations, were those encoding the RNA-binding protein *hfq* (6 subpopulations) and the OM protein *nlpI* (4 subpopulations).

Of note, both loci are components of the *E. coli* core genome, and we surveyed their sequences across a large subset of the isolates profiled here. We determined the *nlpI* and *hfq* sequence for 241 parental VUTI isolates of the following colony biofilm phenotypes: 64 smooth and white, 95 smooth and CR-philic, 32 rugose and CR-philic, 22 dew drop, and 26 peppermint (**Supplementary Data 4**). Both genes were encoded by all isolates with minimal nucleotide and amino acid variability (~99 %+) (Fig. S4). A single amino acid substitution was present in 22/241 strains for *nlpI* (7 F156C and 12 K187R) and 13 strains for hfq (G76S). Likewise, premature *nlpI* truncations were observed in 2 isolates (1 rugose and CR-philic, 1 smooth and CR-philic).

Several of the disrupted loci in emergent VUTI 148 subpopulations have been implicated, directly or indirectly, in the regulation of curli or cellulose in *E. coli*. For example, *eutL* is involved in ethanolamine degradation, while *yciR* encodes a phosphodiesterase of cyclic di-GMP (c-di-GMP) [39–41]. Disruption of these factors could lead to greater EPS production through an increase in available ethanolamine, for the modification of cellulose, or c-di-GMP, which positively regulates EPS production [42–45]. Likewise, mutations in a gene such as *hfq* could impart pleiotropic effects on bacterial growth and physiology, given the diversity of regulatory pathways in which it interacts [45,46]. In this light, and because of previous work exploring the role of these genes in

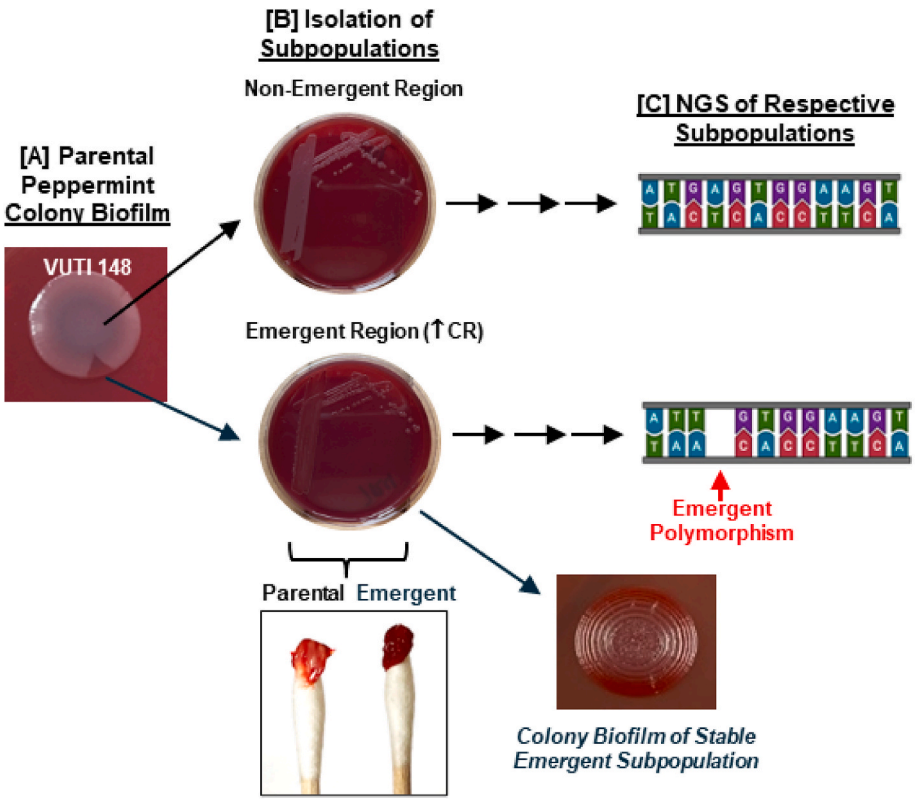

Fig. 4. Schematic Workflow of Peppermint Subpopulation Isolation/Characterization. [A] For VUTI 148, the original peppermint colony biofilm was sampled and sub-cultured from both the predominant parental region and from within the emergent peppermint 'slices' with increased CR uptake. **[B]** Isolation-streaking of the latter yielded agar growth that maintained increased CR uptake over generations (indicated by successive arrows). Further, when emergent populations were propagated as 10-μl inoculated colony biofilms, they demonstrated increased CR uptake and rugosity (relative to the predominant phenotype of parental VUTI 148). **[C]** Finally, the parental population (both original and following subculturing) and the emergent subpopulations were all analyzed via next-generation sequencing to evaluate for the presence of single nucleotide polymorphisms, indels, or larger deletions – ones that were present within the emergent subpopulations, but not any parental samples.

E. coli biofilm formation [47], we chose to focus efforts on the second most frequently disrupted locus, *nlpI*.

Within *E. coli*, the *nlpI* gene is located between the *pnp* (polynucleotide phosphorylase) and *deaD* (dead-box RNA helicase) genes, although not as a discrete operon [48]. It encodes N-terminal motifs required for inner membrane folding and translocation to the OM [49]. The resultant NlpI lipoprotein forms a homodimer anchored to the inner leaflet of the OM, where it can interact with the peptidoglycan layer and additional membrane/periplasmic proteins (via its C-terminus), including the Prc protease [50,51]. This scaffold has been shown to mediate peptidoglycan synthesis and degradation in *E. coli*, while *nlpI* orthologs in other *Enterobacterales* species (*Salmonella typhimurium* and *Erwinia amylovora*) have been implicated in the negative regulation of EPS production [48,52]. Nevertheless, the role of NlpI in the uropathogenesis and biofilm elaboration of *E. coli* remains poorly studied.

3.4. NlpI imparts a negative effect on EPS production in multiple E. coli strain backgrounds

In each of 4 independent subpopulations of VUTI148 with a *nlpI* mutation, the peppermint phenomenon was lost on YESCA-CR agar, with homogenously increased rugosity (particularly in a concentric pattern) and more intense CR staining (Fig. 5A). Three of these mutations (R1.3, R2.3, R2.5) entailed a single-nucleotide substitution in the N-terminal region, while one (R1.2) involved an early 7-nucleotide insertion (Fig. S5). In each case, these changes resulted in massive truncations and presumptive inactivation of resultant protein, with two mutations (R1.3 and R2.3) disrupting even the inner membrane translocation sequence (Fig. S6).

To confirm this interpretation, genetic complementation was performed in all 4 *nlpI* mutants. Each subpopulation was transformed with a high-copy pTrc99A plasmid (under ampicillin selection), encoding wild-type *nlpI* under control of its native promoter. Although transformation with empty vector did not alter the colony biofilm of the subpopulations, complementation with *nlpI* consistently generated a lower-staining background and reemergent peppermint features, reminiscent of parental VUTI148. In fact, intra-strain heterogeneity was more prominent in the context of complementation, with many new subpopulations displaying increased rugosity/CR-uptake (Fig. 5B). Together, these findings indicate that disruption of *nlpI* leads to increased EPS production in VUTI148, implying NlpI as a negative effector of EPS. We next sought to generalize this observation in *E. coli* beyond the wild-type VUTI148 background, by exploring the effect of NlpI inactivation in the UPEC model strain UTI89 (Fig. 5C). At its baseline, UTI89 already generates colony biofilms with intense CR-uptake and prominent concentric rugosity. In this background, a clean deletion of *nlpI* (*ΔnlpI*) further accentuated the phenotype. This included even greater rugosity – with prominent concentric and radial counters – along with a resultant increase in colony biofilm diameter (Fig. 5D). In control analyses, biofilm diameters were not attributable to an increase in cellular replication (Fig. S7). Interestingly, the colony biofilm morphology of UTI89*ΔnlpI* greatly resembled a (previously uncharacterized) construct from a historical *Tn5* transposon library of UTI89 [14], one with a disruption of the *yjcC* phosphodiesterase gene (Fig. 5C-D and S7). This observation is notable as previous findings in *Salmonella* found expression of YjcC positively correlates with NlpI expression [48].

Finally, complementation of the UTI89*ΔnlpI* (with the same pTrc99A-*nlpI* construct employed for VUTI148) abrogated the baseline

Table 1
Increased Congo red emergent events analyzed for genomic polymorphisms: Twenty-six increased-CR emergent events were analyzed for genomic mutations via next generation sequencing techniques. Twenty-two isolated subpopulations contained genomic mutations, some occurring in multiple events as shown by frequency. Asterisk (*/*) indicate shared mutation within one emergent background. Hyphen (~) indicates mutation shared with nlpI emergent. Plus (+) indicates mutation shared with *hfq* emergent.

Gene	Hits	Protein	Function
nlpI	4	Outer membrane lipoprotein	Cell Envelope
prc	1	Tail-specific protease	regulator Proteins
**uvrY*	1	Reponse Regulator	Two Component
**barA*	1	Histidine Kinase	System
hfq	6	RNA-binding protein	Small RNA Binding
dksA	1	RNA polymerase-binding transcription factor	Molecules
yciR	1	Cyclic di-GMP phosphodiesterase	Secondary Signal
icc	1	3′,5′-cyclic adenosine monophosphate phosphodiesterase	Messengers
ompA	1	Peptidoglycan binding protein	Outer membrane
surA	1	Chaperone protein	Proteins
nirB	1	Nitrite reductase (NADH) large subunit	Energy Production/ Other Functions
rne	2	Endoribonuclease	
~*carB*	1	Carbamoyl-phosphate synthase large chain	
**eutL*	1	Ethanolamine degradation	
+*speC*	1	Ornithine decarboxylase	
**ygfT*	1	Putative oxidoreductase	
intergenic region	1	Hypothetical protein	
N/A	4	No mutational differences	

rugosity of UTI89 altogether, but with the striking peppermint-like emergence of new subpopulations (Fig. 5E). Transcriptional analysis indicated the basis of this overcomplemented pattern, with higher expression of *nlpI* in UTI89*ΔnlpI*/p*nlpI* versus the original parental strain (Fig. 5F). Overall, these data for UTI89 reflect the same patterns observed for VUTI148, with *nlpI* expression negatively associated with EPS elaboration, but also a propensity for subpopulation emergence and intra-strain heterogeneity.

3.5. Proteomic and transcriptional effects of nlpI deletion

With this effect of *nlpI*-deletion on UPEC colony biofilms, we next sought to define the corollary impact on other members in the NlpI network. Semi-quantitative tandem mass spectrometry was applied to the outer membrane fraction of UTI89, given its closed genomic sequence with complete protein-encoding coverage [53] (**Supplementary Data 5**). NlpI-derived peptides were only detected at low abundance, even in parental UTI89, with complete abrogation in *ΔnlpI*. Nevertheless, several notable proteins were differentially detected in UTI89-*versus*-*ΔnlpI* (Fig. 6A). As mentioned above, NlpI interacts with Prc to degrade the Spr peptidoglycan endopeptidase [50,54,55].

Accordingly, a higher abundance of Spr would be expected in *ΔnlpI*, from decreased degradation, and this phenomenon was observed prominently. Among other proteins with increased detection for *ΔnlpI* were the YddW outer membrane protein and YhjL/BcsC, the porin of the *E. coli* cellulose transport system [3,56] (Fig. 6A). The latter finding is highly consistent with the observed changes in colony biofilm phenotype**.** A limited number of proteins showed reduced detection in *ΔnlpI*.

One protein not detected in these analyses was CsgA, the extracellular component of curli amyloid. However, this finding is not unexpected for LC-MS-MS approach, given the resistance of these fibers to SDS or protease digestion [57,58]. As a result, we instead utilized RT-qPCR to examine the differential transcription of *csgA* in wild-type and *nlpI*-deleted strains. In UTI89 (wild type *versus ΔnlpI*) strain backgrounds, loss of *nlpI* was associated with upregulated transcription of *csgA* (Fig. 6B). Furthermore, *nlpI*-complementation of the mutant strain returned observed *csgA* transcript levels to the parental baseline (Fig. 6B). Together, these findings connect the *nlpI* associated changes in colony biofilm morphology to a network of physiologic processes that govern the EPS elaboration.

4. Conclusion

Clinical isolates of UPEC of isolates demonstrate tremendous genotypic and phenotypic heterogeneity from strain to strain, including in their biofilm morphology. Notably, EPS components that define *E. coli* colony biofilms, curli and cellulose, are also important virulence factors that help mediate adherence to bladder epithelial cells and urinary catheters [4]. In this study, we observed that a significant minority of urinary *E. coli* isolates generate colony biofilms that consistently develop subpopulations with phenotypic variability, which remain stable after further subculturing. Overall, this phenomenon raises intriguing avenues for further investigation in the area of pathogenesis, including whether intra-strain biofilm heterogeneity impacts a strain's potential for urinary tract virulence or persistence. These studies could help define how this particular manifestation of genotypic/phenotypic heterogeneity (with variable curli/cellulose elaboration) could impart a fitness advantage or impact pathogenicity.

For instance, we envision follow-up work that explore the *in vivo* dynamics of peppermint strains following murine urinary inoculation. These could include experiments that gauge how peppermint isolates evolve *in situ* during infection, and whether parental *versus* emergent subpopulations demonstrate an advantage in the animal bladder, both in and outside the context of antibiotic therapy. Complementary studies could likewise address these issues in the context of human subjects, to clarify how intra-strain biofilm heterogeneity impacts the propensity for recurrent infections. As reported here, we observed an association (from retrospective chart review) between UPEC strains that demonstrate peppermint phenotypes and source-patients with a history of recurrent UTIs. One could hypothesize that this manifestation of intra-strain heterogeneity serves as a bet-hedging mechanism, providing certain strains with an advantage in surviving the host environment and leading to recurrence [59]. More extensive clinical studies are needed, to evaluate this possibility directly, for instance studies larger cohort sizes and prospective follow-up. Of note, other phenotypic examples of intra-strain heterogeneity (outside of biofilm growth) have been recognized for clinical UPEC isolates, with potential implications for pathogenesis or treatment-response. For example, Bermudez et al. recently described the prevalence of heteroresistant UPEC strains during antimicrobial susceptibility testing (AST), specifically the emergence of Fosfomycin non-susceptible subpopulations [60–62]. Like the peppermint biofilm phenomenon reported here, these subpopulations arise due to the real-time emergence of (subsequently stable) genetic mutations.

On a more basic (mechanistic) level, future studies could likewise examine the underlying pressures that predispose certain *E. coli* strains to the emergence of colony biofilm subpopulations in the first place. Despite the focus on *nlpI* within the current manuscript, it was not the only locus in VUTI148 associated with the emergence of intra-strain biofilm heterogeneity. As described in the *Results*, these mutations included other genes connected to the regulation of curli/cellulose. More broadly, many of the mutations arose in genes that may be rationally associated (directly or indirectly) with dynamics at the bacterial cell envelope. These lead us to speculate that VUTI148 (and potentially peppermint strains more broadly) could experience higher baseline levels of cell envelope stress, and that the emergence of subpopulations represents the selection of emergent mutants where such stress is alleviated. For instance, through its interactions with proteins in periplasmic space, NlpI could contribute to total cell-envelope stress, such that *nlpI* mutants experience nullified levels. In general, envelope stress response is primarily regulated by sigma factor E (*rpoE*/σ^{32}) and the two-component system CpxAR, which recognize misfolded outer-membrane

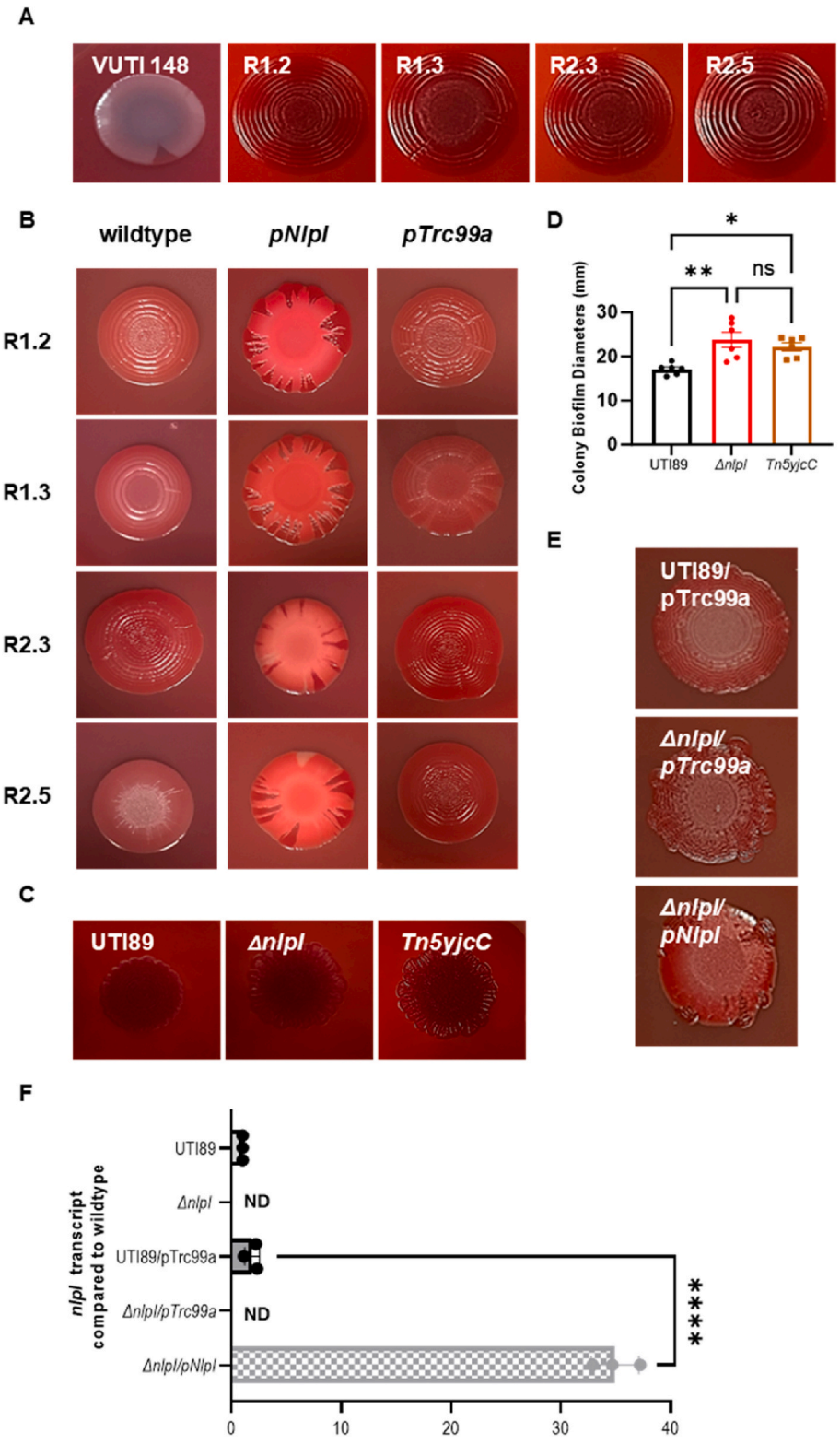

Fig. 5. Mutations in nlpI Alter Colony Biofilm Morphology. [A] The colony biofilm phenotype of parental VUTI148 (peppermint) is compared to the 4 nlpI emergent subpopulations. **[B]** For each of these mutational events in VUTI148, the colony biofilm of the original subpopulation (left) is compared to a nlpI-complemented construct (middle) and an empty vector control (right). **[C]** Within the UTI89 strain-background, the wildtype colony biofilm morphotype is compared to a targeted nlpI-deletion and an *yjcC* mutant from a transposon library. **[D]** The colony diameters of the UTI89 strains of [C] are summarized. **[E]** nlpI-complementation in *UTI89-ΔnlpI* leads to emergence of intrastrain heterogeneity. **[F]** mRNA transcript abundance of *nlpI* in the UTI89 strain-background, assessed via RT-qPCR. Statistical analyses were performed via 1-way Anova (*P < 0.05; **P < 0.01; ****P < 0.0001, NS - not significant; ND - not detected).

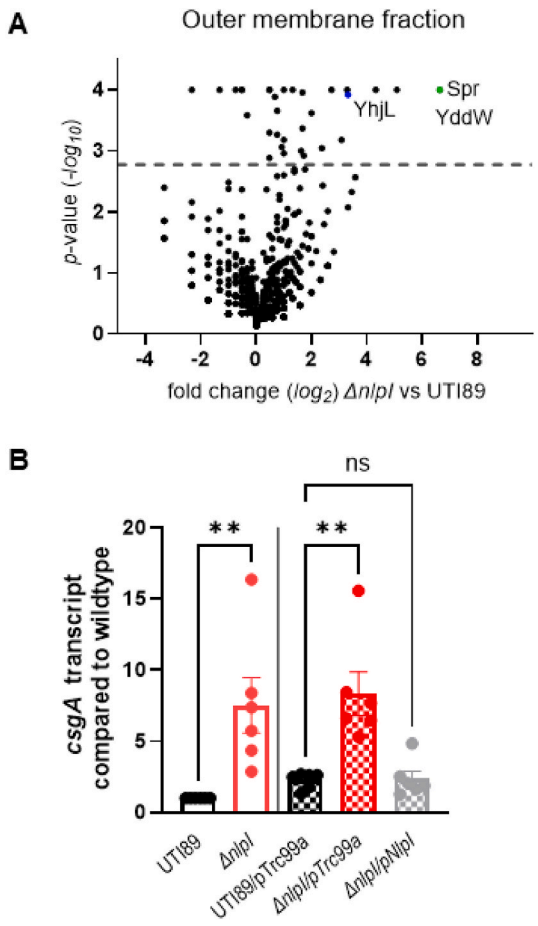

Fig. 6. Proteomic and Transcriptional Analyses of Δ*nlpI* Mutant. **[A]** This volcano plot summarizes the relative abundance of outer-membrane fractionated proteins in UTI89 versus *ΔnlpI*, as assessed through tandem mass spectrometry. The dashed gray line indicates the threshold for statistical significance, via Fisher Extract Analysis ($p < 0.00169$); green dots represent lipoproteins and blue dots represent proteins implicated in extracellular cellulose elaboration. **[B]** This graph depicts the results of RT-qPCR analyses for *csgA* transcript in UTI89 versus *ΔnlpI*, including empty-plasmid controls. Statistical analyses were performed via 1-way Anova (**$P < 0.01$; ns - *not significant*).

proteins and the accumulation of proteins in the periplasm/inner-membrane, respectively [46,63,64]. For instance, it would be of interest to study the impact of NlpI expression on *rpoE* and CpxAR function. In this way, even beyond biofilm regulation, further investigation of NlpI in *E. coli* could represent a valuable avenue to explore the regulation of cell-envelope integrity and maintenance.

Ultimately, one of the most direct implications of intra-strain heterogeneity is it represents a naturally occurring tool for dissecting the genes/proteins that impact biofilm formation. The network of loci implicated in curli/cellulose production is already known to be diverse [45,65,66], and this phenomenon provides a means of defining these components in the context of wild-type strain biology, with the current manuscript focusing on NlpI lipoprotein as a case-in-point example. Within VUTI148, four mutations associated with subpopulation-emergence were (independently) observed in *nlpI*, all involving the introduction of a pre-mature stop codon. These subpopulations each demonstrated increased rugosity and CR uptake compared to the dominant parental phenotype, and a clean deletion of *nlpI* in the model isolate UTI89 (*ΔnlpI*) recapitulated this pattern. Likewise, complementation of *nlpI* reestablished (or in the case of UTI89, established for the first time) the peppermint phenomenon.

Regarding the underlying mechanism by which NlpI influences EPS elaboration, potential steps in this pathway may be inferred from both previous work in *E. coli*, as well as other members of *Enterobacterales* (which encode homologous genes) (Fig. 7) [48,52]. As discussed above, NlpI interacts with the Prc protease, and this complex is responsible for degrading DD-endopeptidase Spr [50,55]. Within *Salmonella*, it has been shown that expression of the YjcC phosphodiesterase (PDE) positively correlates with NlpI/Prc expression [48]. Moreover, back in *E. coli*, YjcC acts as a general negative regulator of EPS production through its cleavage of c-di-GMP [67–69]. Further downstream, as studied in *Erwinia amylovora*, the small RNA *proQ* positively regulates *yjcC* expression in *Erwinia amylovora* [52]. More broadly, the transcription factor CsgD serves as a master regulator of >20 genes during stationary-phase growth, including curli/cellulose-associated loci [6,70,71]. Among intestinal *E. coli* strains, for example, Uhlich et al. observed naturally occurring derivative strains with altered YESCA-CR phenotypes, demonstrating mutations in the promoter region of *csgD*. Therefore, we hypothesize that NlpI-levels could play a countervailing role to the positive regulatory effect of CsgD on curli/cellulose production.

To these ends, future investigations could profile the relative transcript-levels for *nlpI* and *csgD* across diverse clinical isolates of *E. coli*, with cross-comparison to their respective colony biofilm phenotypes. Importantly, such work could help specify the extent of *nlpI* involvement in the organism's natural physiologic network of biofilm elaboration. Through both spontaneous and engineered mutagenesis, the present work clearly demonstrates that NlpI levels exert a prominent impact on a *E. coli* strain's elaboration of EPS. However, additional research could further characterize the extent of NlpI-level variability as a dedicated biofilm regulatory mechanism. Although truncation mutants were observed in a small fraction of parental VUTI isolates (i.e. prior to any subpopulation emergence - Fig. S4), the norm for this species appears to be an intact *nlpI* gene within the core genome. Thus, by defining strain-specific transcript variability, one could evaluate the prominence of *nlpI* among the various genes/proteins that govern biofilm formation *in vivo*.

By incorporating the phenomenon of intra-strain heterogeneity, this manuscript attempts to expand the classes and criteria by which *E. coli* colony biofilms can be evaluated. Looking ahead, future research could continue to expand these paradigms in other important ways. For instance, the underlying method for assigning strains into different categories (i.e. smooth and white, smooth and CR-philic, rugose and CR-philic, dew drop, and peppermint) could evolve beyond the current standard of visual inspection. Admittedly, this approach entails some level of interpretative subjectivity, and we believe future methodologies incorporate pixel-based image analysis and computational evaluation. Toward this goal, we are currently engaged in follow-up work to digitize colony biofilm analysis through colorimetric, topologic, spatial, and temporal parameters. Although this work entails various analytic and statistical intricacies, it could provide a valuable framework to assess colony biofilm phenotypes in a more quantitative manner, while utilizing these categories to define their underlying genetic regulation.

In summary, this work describes the emergence of intra-strain colony biofilm heterogeneity within a substantial minority of UPEC isolates obtained from clinical care. Evaluation of 26 stochastic events in the VUTI148 strain background (via next generation sequencing) identified 22 subpopulations with genomic mutations, including 4 within the outer membrane lipoprotein NlpI. Our characterization of *nlpI* mutants – in both VUTI148 and UTI89 backgrounds – points to this lipoprotein as a negative effector of curli and cellulose in *E. coli*, extending past findings in other *Enterobacterales* species. Overall, these findings highlight the complexity of *E. coli* biofilm regulation, while reporting a wildtype phenomenon that can be exploited to further map these processes.

CRediT authorship contribution statement

Hamilton D. Green: Writing – review & editing, Writing – original draft, Visualization, Validation, Software, Methodology, Investigation,

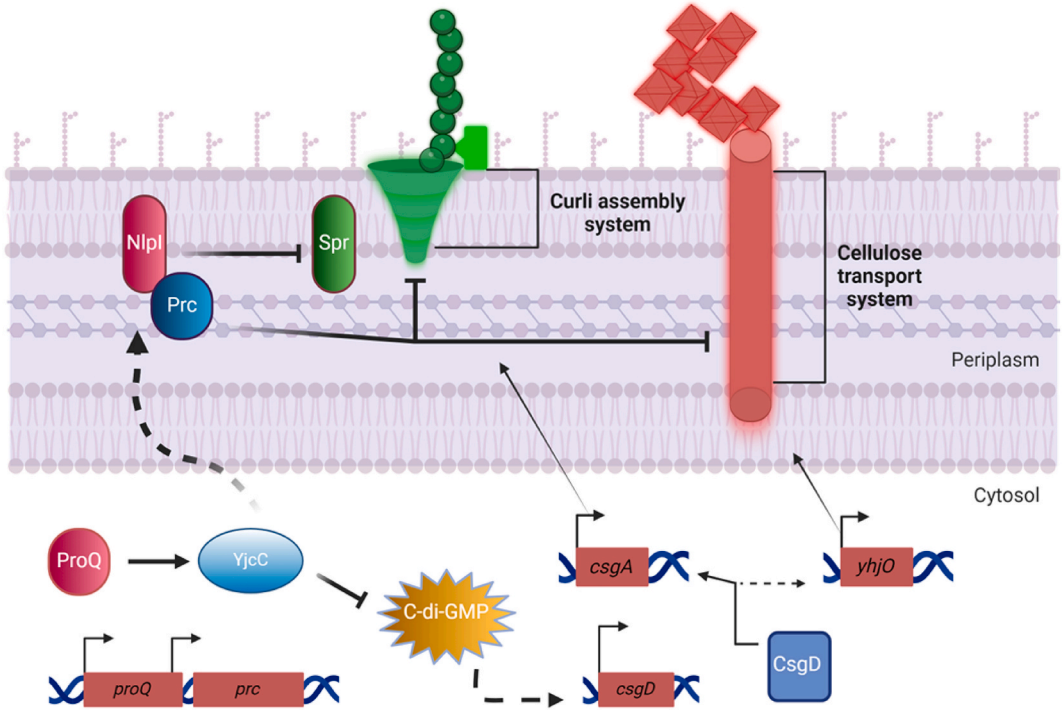

Fig. 7. Proposed Model of NlpI Regulation of Curli and Cellulose. The NlpI network depicted above is a combination of data from the current manuscript and previous literature from other *Enterbacterales* species. NlpI and Prc interact on the inner-leafet of the outer membrane to degrade the lipoprotein Spr. The regulation of the NlpI/Prc network is indirectly controlled by the expression of the small RNA binding molecule *proQ,* which is directly downstream of the *prc* open reading frame. The expression of *proQ* influences the regulation of phosphodiesterase YjcC. YjcC degrades the secondary signaling messenger cyclic-di-GMP, an important signaling factor for the master regulator CsgD. CsgD is a positive transcriptional regulator for curli related genes such as the amyloid adhesive fiber *csgA* and indirectly promotes transcription of cellulose synthase *yhjO*. Solid lines indicate direct interactions, dash lines indicate indirect interactions, and blunt arrows indicate inhibition.

Formal analysis, Conceptualization. **Gerald T. Van Horn:** Writing – review & editing, Supervision, Investigation, Formal analysis, Data curation. **Timothy Williams:** Methodology, Investigation, Formal analysis. **Allison Eberly:** Writing – review & editing, Methodology, Investigation. **Grace H. Morales:** Data curation, Formal analysis. **Robert Mann:** Writing – review & editing, Visualization, Investigation. **Indiana M. Hauter:** Investigation. **Maria Hadjifrangiskou:** Writing – review & editing, Writing – original draft, Validation, Supervision, Resources, Project administration, Methodology, Investigation, Funding acquisition, Formal analysis, Data curation, Conceptualization. **Jonathan E. Schmitz:** Writing – review & editing, Writing – original draft, Supervision, Resources, Project administration, Methodology, Investigation, Funding acquisition, Formal analysis, Data curation, Conceptualization.

Declaration of competing interest

The authors declare the following financial interests/personal relationships which may be considered as potential competing interests: Co-author Maria Hadjifrangiskou currently works for Elsevier's Biofilm's editorial board. If there are other authors, they declare that they have no known competing financial interests or personal relationships that could have appeared to influence the work reported in this paper.

Data availability

Data will be made available on request.

Acknowledgements/FUNDING

The authors would like to thank members of the Hadjifrangiskou and Schmitz laboratories for their thoughtful feedback and input into the current project/manuscript. In addition, thanks are in order for the proteomics core at Vanderbilt University. This work was financially supported by the Center for Personalized Microbiology *(MicroVU)* Trans-Institutional Reinvestment Award, P20 DK123967-01 (to JES and MH), and R21 AI175788 (to MH).

Appendix A. Supplementary data

Supplementary data to this article can be found online at https://doi.org/10.1016/j.bioflm.2024.100214.

References

[1] Mandakhalikar KD, Rahmat JN, Chiong E, Neoh KG, Shen L, Tambyah PA. Extraction and quantification of biofilm bacteria: method optimized for urinary catheters. Sci Rep 2018;8:8069.
[2] Lebeaux D, Ghigo JM, Beloin C. Biofilm-related infections: bridging the gap between clinical management and fundamental aspects of recalcitrance toward antibiotics. Microbiol Mol Biol Rev 2014;78:510–43.
[3] Jeffries J, Thongsomboon W, Visser JA, Enriquez K, Yager D, Cegelski L. Variation in the ratio of curli and phosphoethanolamine cellulose associated with biofilm architecture and properties. Biopolymers 2021;112:e23395.
[4] Hollenbeck EC, Antonoplis A, Chai C, Thongsomboon W, Fuller GG, Cegelski L. Phosphoethanolamine cellulose enhances curli-mediated adhesion of uropathogenic. Proc Natl Acad Sci U S A 2018;115:10106–11.
[5] Serra DO, Richter AM, Hengge R. Cellulose as an architectural element in spatially structured Escherichia coli biofilms. J Bacteriol 2013;195:5540–54.
[6] Prigent-Combaret C, Brombacher E, Vidal O, Ambert A, Lejeune P, Landini P, Dorel C. Complex regulatory network controls initial adhesion and biofilm formation in Escherichia coli via regulation of the csgD gene. J Bacteriol 2001;183:7213–23.
[7] Schiessl KT, Hu F, Jo J, Nazia SZ, Wang B, Price-Whelan A, Min W, Dietrich LEP. Phenazine production promotes antibiotic tolerance and metabolic heterogeneity in Pseudomonas aeruginosa biofilms. Nat Commun 2019;10:762.

[8] Sabir N, Ikram A, Zaman G, Satti L, Gardezi A, Ahmed A, Ahmed P. Bacterial biofilm-based catheter-associated urinary tract infections: causative pathogens and antibiotic resistance. Am J Infect Control 2017;45:1101–5.

[9] Hoiby N, Bjarnsholt T, Givskov M, Molin S, Ciofu O. Antibiotic resistance of bacterial biofilms. Int J Antimicrob Agents 2010;35:322–32.

[10] Ito A, Taniuchi A, May T, Kawata K, Okabe S. Increased antibiotic resistance of Escherichia coli in mature biofilms. Appl Environ Microbiol 2009;75:4093–100.

[11] Martí S, Rodríguez-Baño J, Catel-Ferreira M, Jouenne T, Vila J, Seifert H, Dé E. Biofilm formation at the solid-liquid and air-liquid interfaces by Acinetobacter species. BMC Res Notes 2011;4:5.

[12] Hollenbeck EC, Fong JC, Lim JY, Yildiz FH, Fuller GG, Cegelski L. Molecular determinants of mechanical properties of V. cholerae biofilms at the air-liquid interface. Biophys J 2014;107:2245–52.

[13] Wu C, Lim JY, Fuller GG, Cegelski L. Quantitative analysis of amyloid-integrated biofilms formed by uropathogenic Escherichia coli at the air-liquid interface. Biophys J 2012;103:464–71.

[14] Hadjifrangiskou M, Gu AP, Pinkner JS, Kostakioti M, Zhang EW, Greene SE, Hultgren SJ. Transposon mutagenesis identifies uropathogenic Escherichia coli biofilm factors. J Bacteriol 2012;194:6195–205.

[15] Andersson EK, Bengtsson C, Evans ML, Chorell E, Sellstedt M, Lindgren AE, Hufnagel DA, Bhattacharya M, Tessier PM, Wittung-Stafshede P, Almqvist F, Chapman MR. Modulation of curli assembly and pellicle biofilm formation by chemical and protein chaperones. Chem Biol 2013;20:1245–54.

[16] Thongsomboon W, Werby SH, Cegelski L. Evaluation of phosphoethanolamine cellulose production among bacterial communities using Congo red fluorescence. J Bacteriol 2020;202.

[17] Reichhardt C, Jacobson AN, Maher MC, Uang J, McCrate OA, Eckart M, Cegelski L. Congo red interactions with curli-producing E. coli and native curli amyloid fibers. PLoS One 2015;10:e0140388.

[18] Reichhardt C, McCrate OA, Zhou X, Lee J, Thongsomboon W, Cegelski L. Influence of the amyloid dye Congo red on curli, cellulose, and the extracellular matrix in E. coli during growth and matrix purification. Anal Bioanal Chem 2016;408:7709–17.

[19] Serra DO, Hengge R. Experimental detection and visualization of the extracellular matrix in macrocolony biofilms. Methods Mol Biol 2017;1657:133–45.

[20] Serra DO, Hengge R. Stress responses go three dimensional - the spatial order of physiological differentiation in bacterial macrocolony biofilms. Environ Microbiol 2014;16:1455–71.

[21] Cimdins A, Simm R. Semiquantitative analysis of the red, dry, and rough colony morphology of Salmonella enterica serovar typhimurium and Escherichia coli using Congo red. Methods Mol Biol 2017;1657:225–41.

[22] Uhlich GA, Cooke PH, Solomon EB. Analyses of the red-dry-rough phenotype of an Escherichia coli O157:H7 strain and its role in biofilm formation and resistance to antibacterial agents. Appl Environ Microbiol 2006;72:2564–72.

[23] Giaouris E, Heir E, Desvaux M, Hébraud M, Møretrø T, Langsrud S, Doulgeraki A, Nychas GJ, Kačániová M, Czaczyk K, Ölmez H, Simões M. Intra- and inter-species interactions within biofilms of important foodborne bacterial pathogens. Front Microbiol 2015;6:841.

[24] Dragoš A, Kiesewalter H, Martin M, Hsu CY, Hartmann R, Wechsler T, Eriksen C, Brix S, Drescher K, Stanley-Wall N, Kümmerli R, Kovács Á. Division of labor during biofilm matrix production. Curr Biol 2018;28:1903–1913.e5.

[25] Stewart PS, Franklin MJ. Physiological heterogeneity in biofilms. Nat Rev Microbiol 2008;6:199–210.

[26] Foster PL, Lee H, Popodi E, Townes JP, Tang H. Determinants of spontaneous mutation in the bacterium Escherichia coli as revealed by whole-genome sequencing. Proc Natl Acad Sci U S A 2015;112:E5990–9.

[27] Serra DO, Richter AM, Klauck G, Mika F, Hengge R. Microanatomy at cellular resolution and spatial order of physiological differentiation in a bacterial biofilm. mBio 2013;4:e00103–13.

[28] Beebout CJ, Eberly AR, Werby SH, Reasoner SA, Brannon JR, De S, Fitzgerald MJ, Huggins MM, Clayton DB, Cegelski L, Hadjifrangiskou M. Respiratory heterogeneity shapes biofilm formation and host colonization in uropathogenic Escherichia coli. mBio 2019;10.

[29] Eberly AR, Beebout CJ, Carmen Tong CM, Van Horn GT, Green HD, Fitzgerald MJ, De S, Apple EK, Schrimpe-Rutledge AC, Codreanu SG, Sherrod SD, McLean JA, Clayton DB, Stratton CW, Schmitz JE, Hadjifrangiskou M. Defining a molecular signature for uropathogenic versus urocolonizing Escherichia coli: the status of the field and new clinical opportunities. J Mol Biol 2020;432:786–804.

[30] Murphy KC, Campellone KG. Lambda Red-mediated recombinogenic engineering of enterohemorrhagic and enteropathogenic E. coli. BMC Mol Biol 2003;4:11.

[31] Serra DO, Klauck G, Hengge R. Vertical stratification of matrix production is essential for physical integrity and architecture of macrocolony biofilms of Escherichia coli. Environ Microbiol 2015;17:5073–88.

[32] Uhlich GA, Keen JE, Elder RO. Mutations in the csgD promoter associated with variations in curli expression in certain strains of Escherichia coli O157:H7. Appl Environ Microbiol 2001;67:2367–70.

[33] Morales G, Abelson B, Reasoner S, Miller J, Earl AM, Hadjifrangiskou M, Schmitz J. The role of mobile genetic elements in virulence factor carriage from symptomatic and asymptomatic cases of Escherichia coli bacteriuria. Microbiol Spectr 2023;11:e0471022.

[34] Eng JK, McCormack AL, Yates JR. An approach to correlate tandem mass spectral data of peptides with amino acid sequences in a protein database. J Am Soc Mass Spectrom 1994;5:976–89.

[35] Kohler D, Staniak M, Tsai TH, Huang T, Shulman N, Bernhardt OM, MacLean BX, Nesvizhskii AI, Reiter L, Sabido E, Choi M, Vitek O. MSstats version 4.0: statistical analyses of quantitative mass spectrometry-based proteomic experiments with chromatography-based quantification at scale. J Proteome Res 2023;22:1466–82.

[36] Pfaffl MW. A new mathematical model for relative quantification in real-time RT-PCR. Nucleic Acids Res 2001;29:e45.

[37] Barnhart MM, Chapman MR. Curli biogenesis and function. Annu Rev Microbiol 2006;60:131–47.

[38] Eberly AR, Floyd KA, Beebout CJ, Colling SJ, Fitzgerald MJ, Stratton CW, Schmitz JE, Hadjifrangiskou M. Biofilm Formation by uropathogenic Escherichia coli is favored under oxygen conditions that mimic the bladder environment. Int J Mol Sci 2017;18.

[39] Del Papa MF, Perego M. Ethanolamine activates a sensor histidine kinase regulating its utilization in Enterococcus faecalis. J Bacteriol 2008;190:7147–56.

[40] Solano C, Garcia B, Latasa C, Toledo-Arana A, Zorraquino V, Valle J, Casals J, Pedroso E, Lasa I. Genetic reductionist approach for dissecting individual roles of GGDEF proteins within the c-di-GMP signaling network in Salmonella. Proc Natl Acad Sci U S A 2009;106:7997–8002.

[41] Serra DO, Hengge R. A c-di-GMP-Based switch controls local heterogeneity of extracellular matrix synthesis which is crucial for integrity and morphogenesis of Escherichia coli macrocolony biofilms. J Mol Biol 2019;431:4775–93.

[42] Beloin C, Valle J, Latour-Lambert P, Faure P, Kzreminski M, Balestrino D, Haagensen JA, Molin S, Prensier G, Arbeille B, Ghigo JM. Global impact of mature biofilm lifestyle on Escherichia coli K-12 gene expression. Mol Microbiol 2004;51:659–74.

[43] Weber H, Pesavento C, Possling A, Tischendorf G, Hengge R. Cyclic-di-GMP-mediated signalling within the sigma network of Escherichia coli. Mol Microbiol 2006;62:1014–34.

[44] Collet A, Cosette P, Beloin C, Ghigo JM, Rihouey C, Lerouge P, Junter GA, Jouenne T. Impact of rpoS deletion on the proteome of Escherichia coli grown planktonically and as biofilm. J Proteome Res 2008;7:4659–69.

[45] Kulesus RR, Diaz-Perez K, Slechta ES, Eto DS, Mulvey MA. Impact of the RNA chaperone Hfq on the fitness and virulence potential of uropathogenic Escherichia coli. Infect Immun 2008;76:3019–26.

[46] Vogt SL, Raivio TL. Hfq reduces envelope stress by controlling expression of envelope-localized proteins and protein complexes in enteropathogenic Escherichia coli. Mol Microbiol 2014;92:681–97.

[47] Parker A, Cureoglu S, De Lay N, Majdalani N, Gottesman S. Alternative pathways for Escherichia coli biofilm formation revealed by sRNA overproduction. Mol Microbiol 2017;105:309–25.

[48] Rouf SF, Ahmad I, Anwar N, Vodnala SK, Kader A, Römling U, Rhen M. Opposing contributions of polynucleotide phosphorylase and the membrane protein NlpI to biofilm formation by Salmonella enterica serovar Typhimurium. J Bacteriol 2011;193:580–2.

[49] Smithers L, Olatunji S, Caffrey M. Bacterial lipoprotein posttranslational modifications. New insights and opportunities for antibiotic and vaccine development. Front Microbiol 2021;12:788445.

[50] Tadokoro A, Hayashi H, Kishimoto T, Makino Y, Fujisaki S, Nishimura Y. Interaction of the Escherichia coli lipoprotein NlpI with periplasmic prc (tsp) protease. J Biochem 2004;135:185–91.

[51] Snyder WB, Davis LJ, Danese PN, Cosma CL, Silhavy TJ. Overproduction of NlpE, a new outer membrane lipoprotein, suppresses the toxicity of periplasmic LacZ by activation of the Cpx signal transduction pathway. J Bacteriol 1995;177:4216–23.

[52] Yuan X, Eldred LI, Kharadi RR, Slack SM, Sundin GW. The RNA-binding protein ProQ impacts exopolysaccharide biosynthesis and second messenger cyclic di-GMP signaling in the fire blight pathogen Erwinia amylovora. Appl Environ Microbiol 2022;88:e0023922.

[53] Chen SL, Hung CS, Xu J, Reigstad CS, Magrini V, Sabo A, Blasiar D, Bieri T, Meyer RR, Ozersky P, Armstrong JR, Fulton RS, Latreille JP, Spieth J, Hooton TM, Mardis ER, Hultgren SJ, Gordon JI. Identification of genes subject to positive selection in uropathogenic strains of Escherichia coli: a comparative genomics approach. Proc Natl Acad Sci U S A 2006;103:5977–82.

[54] Jeon WJ, Cho H. A cell wall hydrolase MepH is negatively regulated by proteolysis involving prc and NlpI in. Front Microbiol 2022;13:878049.

[55] Singh SK, Parveen S, SaiSree L, Reddy M. Regulated proteolysis of a cross-link-specific peptidoglycan hydrolase contributes to bacterial morphogenesis. Proc Natl Acad Sci U S A 2015;112:10956–61.

[56] Romling U. Molecular biology of cellulose production in bacteria. Res Microbiol 2002;153:205–12.

[57] Zhou Y, Smith DR, Hufnagel DA, Chapman MR. Experimental manipulation of the microbial functional amyloid called curli. Methods Mol Biol 2013;966:53–75.

[58] Collinson SK, Emödy L, Müller KH, Trust TJ, Kay WW. Purification and characterization of thin, aggregative fimbriae from Salmonella enteritidis. J Bacteriol 1991;173:4773–81.

[59] Grimbergen AJ, Siebring J, Solopova A, Kuipers OP. Microbial bet-hedging: the power of being different. Curr Opin Microbiol 2015;25:67–72.

[60] Bermudez TA, Brannon JR, Dudipala N, Reasoner S, Morales G, Wiebe M, Cecala M, DaCosta M, Beebout C, Amir O, Hadjifrangiskou M. Raising the alarm: fosfomycin resistance associated with non-susceptible inner colonies imparts no fitness cost to the primary bacterial uropathogen. Antimicrob Agents Chemother 2024;68:e0080323.

[61] Hurst MN, Beebout CJ, Hollingsworth A, Guckes KR, Purcell A, Bermudez TA, Williams D, Reasoner SA, Trent MS, Hadjifrangiskou M. The QseB response regulator imparts tolerance to positively charged antibiotics by controlling metabolism and minor changes to LPS. mSphere 2023;8:e0005923.

[62] Silver LL. Fosfomycin: mechanism and resistance. Cold Spring Harb Perspect Med 2017;7.

[63] Danese PN, Silhavy TJ. The sigma(E) and the Cpx signal transduction systems control the synthesis of periplasmic protein-folding enzymes in Escherichia coli. Genes Dev 1997;11:1183–93.

[64] Marles-Wright J, Lewis RJ. Stress responses of bacteria. Curr Opin Struct Biol 2007; 17:755–60.
[65] Palaniyandi S, Mitra A, Herren CD, Lockatell CV, Johnson DE, Zhu X, Mukhopadhyay S. BarA-UvrY two-component system regulates virulence of uropathogenic E. coli CFT073. PLoS One 2012;7:e31348.
[66] Justice SS, Lauer SR, Hultgren SJ, Hunstad DA. Maturation of intracellular Escherichia coli communities requires SurA. Infect Immun 2006;74:4793–800.
[67] Klauck G, Serra DO, Possling A, Hengge R. Spatial organization of different sigma factor activities and c-di-GMP signalling within the three-dimensional landscape of a bacterial biofilm. Open Biol 2018;8.
[68] Romling U, Galperin MY, Gomelsky M. Cyclic di-GMP: the first 25 years of a universal bacterial second messenger. Microbiol Mol Biol Rev 2013;77:1–52.
[69] Ma Q, Yang Z, Pu M, Peti W, Wood TK. Engineering a novel c-di-GMP-binding protein for biofilm dispersal. Environ Microbiol 2011;13:631–42.
[70] Ogasawara H, Yamamoto K, Ishihama A. Role of the biofilm master regulator CsgD in cross-regulation between biofilm formation and flagellar synthesis. J Bacteriol 2011;193:2587–97.
[71] Zakikhany K, Harrington CR, Nimtz M, Hinton JC, Römling U. Unphosphorylated CsgD controls biofilm formation in Salmonella enterica serovar Typhimurium. Mol Microbiol 2010;77:771–86.